International Specialty Conference on Cold-Formed Steel Structures

(1988) - 9th International Specialty Conference on Cold-Formed Steel Structures

Nov 8th, 12:00 AM

Structural Behaviour of a Stressed Arch Structural System

Peter W. Key

Chris Olsen

Gregory J. Hancock

Recommended Citation

STRUCTURAL BEHAVIOUR OF A STRESSED ARCH STRUCTURAL SYSTEM

Gregory Hancock[1], Peter Key[2] and Chris Olsen[3]

Summary

The paper describes a structural system consisting of plane arched trusses composed of cold-formed circular and square hollow sections. The unique feature of the structural system is the way the arches are erected without the use of cranes or scaffolding but by the use of a post-tensioning process. A prestressing cable passing through the bottom chord of the truss is stressed so that predetermined gaps in the bottom chord close to allow the chord to shorten thus producing upward curvature of the truss into an arch shape.

During the uplift of the truss, the top chord is curved in negative bending. For some highly curved structures, the top chord may be plastically deformed during the erection procedure. In addition, the top chord must support the axial compressive force in equilibrium with the tendon force in the bottom chord. The purpose of this paper is to describe a series of tests which were performed on sub-assemblages of the stressed arch at the University of Sydney, on behalf of Strarch International Ltd., to determine the effect of the negative curvature of the top chord on its axial capacity. A nonlinear analysis model of a length of top chord between node points is also described and compared with the test strengths.

[1]   Associate Professor, School of Civil and Mining Engineering,
       University of Sydney, Australia, 2006.

[2]   Postgraduate Student, School of Civil and Mining Engineering,
       University of Sydney, Australia, 2006.

[3]   Director, Research, Strarch International Ltd., P.O. Box 6304
       Melbourne, Australia, 3004.

273

1. INTRODUCTION

A recent development in steel structures in Australia is a structural system produced by Strarch International Limited of Melbourne, Victoria, Australia. The system consists of prefabricated truss segments which are erected without scaffolding or cranes but by the use of internal prestressing cables.

The erection procedure involves the assembly of the primary load–carrying steel trusses of a building at ground level, followed by a post–tensioning process to lift the structure into its final working configuration. Prefabricated truss segments, consisting of a cold–formed square hollow section top chord and a twin circular hollow section bottom chord with sliding joints, are delivered to site and bolted together at ground level to form a complete truss, as depicted in Fig. 1(a). All of the trusses needed to form the complete building are prepared in this way. Purlins, cladding and services are fixed to the trusses while the structure is at ground level so as to form a complete roof structure. Steel prestressing wires drawn through the twin bottom chord tubes are then tensioned, causing the gaps in the sliding joints in each bottom chord panel to close up, and lifting of the structure into an arch configuration. This process induces bending and compression in the top chord. The final shape (see Fig. 1(b)) is dictated by the predetermined initial gaps in the sliding joints. Fixing of the columns and grouting of the bottom chord prestressing wires complete the erection procedure.

The resulting structure is claimed to be substantially cheaper to fabricate and erect than conventional truss structures spanning the same area. Structures up to 60 metres have been built successfully and larger spans are currently being designed.

The erection process causes the top chord to curve upwards. For low–rise structures, the curvature of the top chord, coupled with the axial thrust generally produces elastic deformation of the chord. However, for high–rise structures, the top chord may undergo plastic deformation during the erection process. Construction and testing of a full scale frame (Olsen 1988, University of Melbourne 1988, University of Sydney 1988) and the safe construction of many other full scale frames has indicated that the structure can withstand the combination of axial force and moment present in the top chord after erection and under live load.

The paper describes a detailed experimental research program, which has been performed at the University of Sydney (September 1987, October 1987) to determine the strength of the top chord when subjected to combined erection curvature and compression. The tests were performed on sub–assemblages composed of top chord, web and bottom chord members. The main purpose of this research program was to determine the behaviour of the top chord under axial compression and to demonstrate that the combinations of moment and axial thrust present in the top chord are within safe limits. A simple nonlinear analysis model of a segment of the top chord between adjacent panel points is also described to demonstrate the importance of the boundary conditions at the end of a segment on its ultimate strength.

2. STATICS OF THE STRESSED ARCH DURING ERECTION AND LOADING

During erection, the support at one end of the structure is free to slide and so the structural support system drawn in Fig. 2(a) can be assumed. The support reactions are statically determinate in this system. For the purpose of a simplified analysis, the structure shown in Fig. 2(a) has been assumed to be subjected to a

uniformly distributed dead load (W_D) acting downwards over the full span. A simple static analysis can be performed to determine the axial thrust (C) in the top chord as shown in Fig. 2(b).

The negative moment (M_{TC}) induced in the top chord by the erection procedure is not statically determinate but is a function of the applied curvature and the flexural rigidity of the chord section. However, the magnitude of M_{TC} is usually small compared with the moment produced by the dead load ($W_D L^2/8$) and so the axial thrust (C) is statically determinate to within a small error. As a consequence of the erection process, the full length of the bottom chord is in tension under the action of dead load alone.

After erection of the structure, the column bases are normally locked into position so that the structure becomes statically indeterminate under the action of live load. For downwards live load over the full span, this will induce superimposed compression in the bottom chord near the eaves. However, the bottom chord will not be in net compression until the additional compressive force resulting from live load exceeds the tension force in the bottom chord resulting from dead load during erection. In many practical cases, the bottom chord remains in net tension even under the action of downwards live load such as snow load.

On completion of erection, the top chord is subject to the combined axial force (C) and negative bending moment (M_{TC}). Under the action of downwards live load, additional axial thrust will occur in the top chord near the apex. The moment (M_{TC}) is unlikely to change substantially under working values of the live load unless the whole structure deforms significantly under the effect of live load. However, if the top chord is subjected to a load which causes it to approach its ultimate limit state, the moment and its distribution in the top chord will begin to alter significantly from its value and distribution after erection as the chord member deforms in its plane between the structure panel points. This phenomenon will be demonstrated in the panel tests described in this paper.

3. TEST PROGRAM

3.1 Test Configuration

The purpose of the tests was to determine the effect of the curvature applied during erection on the compressive strength of the top chord. A panel test rig which could apply both axial thrust and curvature to a test panel was required. The test rig used is shown in Fig. 3 with a typical test panel located in it. The rig consisted of a 2000 kN (200 tonne) servo-controlled hydraulic jack located in a reaction frame. The test panel was located between pinned spherical bearings at either end of the rig. An extensometer was used to measure shortening between the pinned bearings for the purpose of providing extension control rather than load control of the test. The test rig was the same as that used to test the rectangular hollow sections described by Key, Hasan and Hancock (1988) and the welded I-sections described by Davids and Hancock (1986).

Each test panel was firstly subjected to applied curvature, shown as Stage 1 in Fig. 4, using the small hydraulic jack shown in the photo in Fig. 5(a). A curved panel after Stage 1 is shown in Fig. 5(b). The bottom chord length was then fixed. Stage 2 consisted of applying axial force P_j along the line joining the pinned bearings using the servo-controlled jack as shown in Fig. 4.

In a prototype structure, the line of force would be directed between the panel points. However, in the test rig, the line of force is between the pinned bearings.

This changed line of action of the force would have induced additional forces in the web and bottom chord members which would not occur in a prototype structure. Consequently, the length of panel which could be tested was limited. However, for the panel lengths tested, the changed line of action of the force is unlikely to have had any significant effect on the top chord behaviour.

3.2 Test Panel Geometry

Two different types of panels were tested to investigate different aspects of the top chord behaviour. Panel Type A, shown in Fig. 6(a), was used to investigate the variation of both the top chord strength and the overload interaction between two adjacent sections of top chord with different levels of initial erection curvature applied by means of the bottom chord and web members. For this panel type, the curvature in the top chord would be a maximum at the centre and would approach zero at the pinned ends after Stage 1.

Panel Type B shown in Fig. 6(b) was used to develop a uniform curvature along the full length of the central section of its top chord in order to investigate the effect of this curvature on the nonlinear behaviour and the load capacity of the top chord. The curvature at the pinned ends of the top chord would approach zero as for the Panel Type A.

The test panel numbers, types (A or B), dimensions and top chord section sizes are set out in Table 1 using the symbols defined in Fig. 6. All tests had a top chord consisting of a cold-formed square hollow section of overall dimensions 152 × 152 mm. However, the nominal thicknesses of the sections varied from 4.9 mm for the test Panels SP1 – SP9 to 6.3 mm for Panel SP10 and 9.5 mm for Panel SP11. The mean measured thicknesses of the test specimens was 4.97 mm, 6.18 mm and 9.46 mm. The material properties, including the stress–strain curves of the corners and flats of the sections produced by the same manufacturer, have been presented in Key, Hasan and Hancock (1988). The bottom chord and web members for panels SP1 – SP10 were 48 mm O.D. × 4.0 mm thick circular hollow sections. The web members of Panel SP11 were 60 mm O.D. × 3.6 mm thick circular hollow sections, and the bottom chord consisted of two lengths of channel welded in position after curvature had been applied to the top chord.

3.3 Instrumentation

The applied load and axial deformation of the top chord were measured using the control system of the servo–controlled hydraulic jack. Displacement transducers were located at a number of positions along the top chord to measure lateral displacement. In addition, pairs of strain gauges were located at certain positions along the top chord to allow curvature to be determined. The positions of the transducers and strain gauges are shown in Fig. 6. Panels SP1 and SP2 only had Transducer No. 1 and Strain Gauge Pair No. S1. Panel SP9 did not have Transducer Nos. T4 and T5 and Strain Gauge Pair No. S4. All strain gauges and transducers involved in the testing were connected to a SPECTRA multi–channel data acquisition system which allowed almost simultaneous readings of all channels at any load level.

Since the test panels became statically indeterminate when the bottom chord sliding joints were locked, it was necessary to measure the redundant force in the lower chord during testing to allow determination of the forces in each member. For this purpose, a length of SHS section was strain gauged and calibrated for use as a load cell. This load cell was located in the bottom chord during the tests of Panels SP1 – SP8.

3.4 Test Procedure

After positioning the panel in a horizontal plane so that the top chord was approximately concentric with the loading platens of the test rig, a nominal axial load of 10 kN was applied to the top chord to maintain its concentricity. Initial readings were then taken using the instrumentation described in 3.3. The bottom chord jacking arrangement was then used to simulate closing of the gap in the bottom chord. This was done in stages with instrumentation readings being taken after each stage up to the required curvature. The bottom chord load cell was then locked in position. This completed the first stage of the test procedure. Panels SP1 – SP8 were each given different amounts of initial curvature corresponding to differences in the lateral deflection readings (δ in Fig. 4) The initial values of curvature measured at Strain Gauge Locations No. S1 and S2 are given in Table 2. Panel SP8 was initially curved up to the point where local buckling occurred on the inside concave face of the top chord at strain gauge location S1.

The second stage of testing involved application of load by the 2000 kN jack until failure occurred. Axial load was applied in increments of 50 kN, with readings of all instrumentation taken after each increment. Out–of–plane column buckling of the top chord was prevented by placing the top chord between the loading platens with a small nominal eccentricity to induce initial deflections in the downwards direction. A system of blocks and metal wedges was used to restrain the top chord from further movement in this direction during load testing.

3.5 Stub Column Test

A stub column test was performed on a 500 mm length of 152 × 152 × 4.9 mm SHS from the same material used for the Panels SP1 – SP9. The test was performed following the procedures described in Johnston (1976). A maximum axial load of 1170 kN was obtained.

3.6 Test Results

The maximum loads applied by the jack (P_j) are given in Table 2. The load in the bottom chord (P_b) at the ultimate load in the test is also given in Table 2. Hence the net load in the top chord (P) at ultimate is given both in kN and as a percent reduction below the stub column strength. The maximum reduction measured was 35 percent below the stub column strength for Panel SP7.

The mode of failure of the test panels was not the same for all tests. Panel SP1 developed a local buckle in the top chord near Gauge Location S1 after the maximum load had been reached. Panels SP2 – SP4 and SP6 developed local buckles in the vicinity of Gauge Location S3 after the maximum load had been reached. Panel SP5 buckled in the bottom chord before the maximum capacity of the top chord had been reached. Panel SP7 developed an out–of–plane buckle of the bottom chord just after the maximum load in the top chord had been reached. Panel SP9 developed a local buckle in the top chord in the end segment. Panel SP10 developed a local buckle in the web member and Panel SP11 failed by plastic bending of the top chord in the end segment with a general failure of the whole web member/bottom chord system. The failure of Panels SP10 and SP11 was much more ductile than those for Panels SP1 – SP7 and SP9. Panels SP1 – SP9 all had a comparatively thin–walled top chord section with a w/t for the flat faces of 26.0 whereas Panels SP10 and SP11 had thicker walled sections with w/t values for the flat faces of 19.1 and 11.0 respectively.

The load–curvature plots for Panels SP10 and SP11 are given in Figs. 7(a) and (b) respectively. The lateral–deflection profiles for Panels SP10 and SP11 are given in Figs. 8(a) and 8(b) respectively. For Panel SP10, the maximum initial curvature occurred at Gauge Location S1. However, as the load was increased towards the maximum, the curvature at Gauge Location S1 reduced whereas those at Locations S2 and S3 increased with bending failure occurring in the vicinity of S3. The lateral–deflection profile of Panel SP10 shows that the pinned end allowed the segment of the panel to deform mainly towards that end with the centre of the panel being restrained by the adjacent segment. Hence the failure of the instrumented segment of Panel SP10 demonstrates the mode of failure of a beam–column with a moment applied at one end and pinned at the other. As the maximum load of the panel was reached, the curvature and hence moment at the restrained end of the panel reduced whereas that in the vicinity of the pinned end increased as a consequence of rotation of the pinned end.

For Panel SP11, the curvature was reasonably uniform initially along the central segment as shown in Fig. 7(b). However, as the maximum load was approached, the curvature towards the centre of the panel increased whereas that towards the ends decreased. The deflected profile in Fig. 8(b) demonstrates the effect of end restraint on the central segment and the reversal of curvature towards its ends.

For the case of both Type B panels (SP9 and SP11), failure occurred in a shorter end segment rather than the longer central segment probably as a result of the effect of the pinned end. This is clearly demonstrated in Fig. 8(b) where the midpoint curvature in the central segment increases until close to the maximum load at which point the curvature in the short end segment increases dramatically prior to failure. The central segment was restrained at both ends and therefore had a higher load capacity. For all of the Panel Type A tests, the effect of the pinned ends was to reduce the load capacity of the panels below those in the prototype structure which would normally have restraint at both ends as in the central segments of the Type B panels.

3.7 Load–Curvature Plot

A graph of maximum load versus the initially applied curvature is shown for Panels SP3 – SP7 and SP9 in Fig. 9. For Panels SP3 – SP7, the curvature at the centre of the instrumented segment at Gauge Location S2 has been used in plotting the points on Fig. 9 since it is considered that this is an approximate mean value for the segment. The rate of reduction with increasing initial curvature appears to decrease as the curvature is increased. The Panel SP9 test result is slightly above those for Panels SP3 – SP7 probably as a result of the shorter length of the end segment which failed when compared with the similarly restrained end segments in Panels SP3 – SP7. The load carried by the bottom chord (P_b) for Panel SP9 was not measured and so has not been subtracted from the applied load (P_j).

Full details of the tests are given in an Investigation Report (University of Sydney – September 1987).

4. NONLINEAR BEHAVIOUR OF CHORD SEGMENT

4.1 Nonlinear Analysis Method

The large deformation elastic–plastic analysis of a complete structural system is complex and computer intensive if its nonlinear behaviour is to be modelled realistically. Hence, for the purpose of determining the limiting behaviour of the top chord, an analysis was developed to study a segment only of the chord

member between panel points when subjected to the limiting boundary conditions of pinned and fixed ends.

The method of nonlinear analysis chosen was the Influence Coefficient Method (ICM) presented by Chen and Atsuta (1977). A computer program implemented by Davids and Hancock (1987) to study the buckling behaviour of thin-wallled I-section columns undergoing local buckling was modified to accommodate the particular material and section characteristics of the tubular top chord of the stressed-arch frame.

In the Influence Coefficient Method, the beam-column is modelled as a series of nodes at which equilibrium is sought by an iterative procedure involving the nodal displacements. A beam-column under study is shown in its discretised form in Fig. 10. An axial load P can be applied at eccentricity e from the line joining the centreline of the ends, end moments M_1 and M_2 can be applied, and lateral forces (F_i) can be applied at each node (i). The end support conditions allow axial displacement, but no lateral displacement. End rotational restraint can be specified as pinned, fixed or with specified elastic rotational restraint.

Material nonlinearity can be accounted for by using moment-curvature data specified in a matrix format. In this approach, the axial and flexural behaviour of a cross-section is summarised in two matrices. One matrix contains the axial force in the cross-section as a function of applied curvature and axial strain. The second matrix contains the moment on the section as a function of applied curvature and axial strain. The ICM analysis makes reference to these matrices for the current curvature and axial force conditions to set up the equilibrium equations, as set out in Davids and Hancock (1987).

The ICM analysis uses an incremental approach in which the full load-deformation history of the beam-column is obtained by applying increments of axial load and solving for the deformed position. The analysis of a length of top chord between panel points presents a special problem in that the structure has a degree of axial strain and precurvature imposed by the erection process before further loading. The ICM analysis presented by Davids and Hancock (1987) was modified to allow precurvature to be applied. The first increment of load consisted of application of equal and opposite end moments to the pin-ended column, where the magnitude of the moments was adjusted to give the required degree of precurvature. The boundary conditions were then altered to restraints, such as fixed at both ends, and the analysis then continued with increments of axial load until the ultimate capacity was reached. The full details of the analytical techniques are given in an Investigation Report (University of Sydney, November 1987).

4.2 Moment and Axial Force Matrices for Yielded Cross-Sections

The program MQCURV used to generate the matrices of moment and axial force at different levels of applied axial strain and curvature is a modification of a program developed by Bridge (1979). The program divides the cross-section into a number of small elemental areas. Applied curvature and axial strain on a section result in an applied strain at the centre of each element. The residual strain at each element is added to the applied strain and the corresponding stress is determined using the chosen stress-strain relationship. The axial force and bending moment resisted by the section are then found by integrating the stresses in the elemental areas over the whole section. The analysis is equivalent to presuming that unloading returns along the original stress-strain curve and does not take place elastically from the yield surface.

The material stress–strain relationships and the residual stress distributions used in the analysis described in this paper are the same as those described by Key, Hasan and Hancock (1988) for cold–formed square hollow sections produced by the same manufacturing process. The cross–section analysis allowed for the variation of yield stress around the cross–section, particularly the modified stress–strain characteristics in the highly worked corners. The cross–section analysis also allowed for the through–thickness residual stress distribution which was measured experimentally at Cambridge University, U.K. using a spark erosion technique as described by Scaramangas (1984). The technique was applied to a sample of Australian produced cold–formed square hollow section which was sent to Cambridge for testing (Cambridge University 1985).

4.3 Results of Nonlinear Analysis

The nonlinear analysis was performed for a segment of top chord of section size 152 mm × 152 mm × 4.9 mm, and panel point spacing of 2 metres. This geometry is the same as Panel Tests SP1 – SP8. The analysis was used to study two cases, namely:

(a) a uniform applied curvature in the first increment followed by axial loading of a member with pinned ends (called Case 1), and

(b) a uniform applied curvature in the first increment followed by axial loading with both ends fixed against rotation (called Case 2).

These two cases represent the extremes of end fixity to which a panel length of top chord is likely to be subjected. For both cases, a range of initial curvatures was applied before axial loading.

The axial load versus central deflection results for Case 1 are plotted in Fig. 11(a). Results are shown for a range of initial curvatures. The ultimate load capacity corresponds to a significant curvature increase at centre span, and the formation of a hinge leading to a plastic mechanism.

The axial load versus central deflection results for Case 2 are plotted in Fig. 11(b). Results are shown for a range of initial curvatures as for Case 1. The results show a significant change in stiffness corresponding to the formation of a plastic hinge at centre span. However, this hinge does not terminate the load capacity and the member with fixed ends still has a significant reserve capacity. It is not until plastic hinges have formed at each end that the ultimate load is reached.

The results of the ICM analysis have been plotted for comparison with the panel test results on Fig. 9. It is clear that the Case 1 and Case 2 analytical results form lower and upper bounds respectively to the test results. This is probably a consequence of the test boundary conditions which are essentially fixed at one end and pinned at the other. It can be hypothesised that the prototype structure would be closer to Case 2 with fixed boundary conditions at each end. However, the degree of interaction between adjacent segments is not known at this stage and so further nonlinear analyses of longer lengths of frame will be required. A project in which a nonlinear finite element analysis will be used to study an extended length of frame is currently underway at the University of Sydney.

Of greater significance is the amount by which the test results exceed the Case 1 analyses. For segments subjected to greater curvatures, the test strengths appear to reach a plateau whereas the Case 1 analysis results continue to decrease. This difference explains why full scale frames continue to carry axial load even after

plastic straining of the top chord caused by erection curvature. Simple code predictions (AISC 1986, SAA 1981) are normally based on the Case 1 model and indicate that the top chord has very little axial capacity when the values of erection curvature are high.

The test results and analyses reported in this paper are for top chord segments with overall slenderness between panel points of approximately 33.5. For higher values of column slenderness, further investigation of the nonlinear behaviour is required. A research program to investigate the effect of column slenderness is currently underway at the University of Sydney.

5. CONCLUSIONS

A series of tests on panels taken from stressed arch frames has been described. The unique erection procedure of the stressed arch frames has been modelled in the panel tests. The purpose of the tests was to determine the effect of erection curvature on the compressive strength of the top chord. For the column slenderness of 33.5 chosen, which is typical of frames of this type, the maximum reduction in the column strength capacity below the stub column strength capacity was approximately 35 percent.

A nonlinear analysis model for a segment of top chord was described. The nonlinear analysis accounted for the material properties commonly found in cold-formed square hollow sections. The analysis demonstrated that the top chord capacity was sensitive to initially applied curvature if the segment was supported by pinned ends, but was much less sensitive to initially applied curvature if the segment was supported by fixed ends. The panel tests were found to lie approximately midway between these two limiting sets of analyses.

6. ACKNOWLEDGEMENTS

The authors are grateful to Strarch International Ltd for permission to publish test results of their proprietary frame sections.

7. APPENDIX – REFERENCES

American Institute of Steel Construction, Load and Resistance Factor Design Specification for Structural Steel in Buildings, AISC, Chicago, Sept.

Bridge, R.Q. (1979), "Large Deflection Analysis of Portal Frames", Civil Engineering Transactions, Institution of Engineers, Australia, Vol. CE21, No. 2, Sept.

Cambridge University (1985), "Residual Stress Analysis for University of Sydney on Specimen Plate Cut from 254 × 254 × 6.3 SHS", Private Report.

Chen, W.F. and Atsuta, T. (1977), Theory of Beam–Columns, Vol.2 "Space Behaviour and Design", McGraw–Hill, New York.

Davids, A.J. and Hancock, G.J. (1986), "Compression Tests of Long Welded I–section Columns", J. Struct Eng., ASCE, Vol.112, No. ST10, Oct, pp 2281–97.

Davids, A.J. and Hancock, G.J. (1987) "Nonlinear Elastic Response of Locally Buckled Thin-walled Beam-columns", Thin-walled Structures, Vol. 5, No. 3 pp 211–226.

Key, P.W., Hasan, S.W. and Hancock, G.J. (1988), "Column Behaviour of Cold-Formed Hollow Sections", J. Struct. Eng., ASCE, Vol. 114, No. ST2, Feb., pp 390-407.

Olsen, C.J. (1988), "The Big Summer Tests", Metal Building News, Journal of the Metal Building Products Manufacturer's Association, Australia, March, p11.

Scaramangas, A. (1984), "Residual Stresses in Girth Butt Welded Pipes:- Experimental Techniques", Technical Report, CUED/D-Struct/TR.108, Cambridge University.

Standards Association of Australia (1981), Steel Structures Code, AS1250.

University of Melbourne (1988), "Load Tests of a 30m Span Strarch at High Technology Industrial Park, Craigieburn, Victoria, Investigation Report, No. ST2/88.

University of Sydney (1988), "Strain Gauge Instrumentation of a Strarch Frame during Erection and Load Testing", Test Record, School of Civil and Mining Engineering, No. T451, February.

University of Sydney (1987), "Strarch Panel Tests to Determine Top Chord Strength", Investigation Report, School of Civil and Mining Engineering, No. S621, September.

University of Sydney (1987), "Theoretical Analysis of Strarch Top Chord", Investigation Report, School of Civil and Mining Engineering, No. S630, November.

University of Sydney (1987), "Strarch Panel Test SP11", Test Record, School of Civil and Mining Engineering, University of Sydney,No. T447, October.

TABLE 1 – TEST PANEL TYPE AND DIMENSIONS

Panel No.	Panel Type	Top Chord Size (mm)	Dimensions (mm) defined in Fig. 6						
			x_1	x_2	x_3	x_4	x_5	x_6	x_7
SP1, SP2	A	152×152×4.9 SHS	2000	150	2000	–	150	–	–
SP3– SP8	A	152×152×4.9 SHS	2000	150	2000	667	150	650	800
SP9	B	152×152×4.9 SHS	2000	150	2000	1000	150	1000	–
SP10	A	152×152×6.3 SHS	1700	150	1700	567	150	630	680
SP11	B	152×152×9.5 SHS	3000	150	2900	1500	150	1500	750

TABLE 2 – INITIAL CURVATURES AND MAXIMUM LOADS

Panel No.	Initial Curvature at S1 $\times10^{-6}mm^{-1}$	Initial Curvature at S2 $\times10^{-6}mm^{-1}$	Initial Curvature at S3 $\times10^{-6}mm^{-1}$	Maximum Jack Load P_j(kN)	Bottom Chord Load P_b(kN)	Nett Load Top Chord P(kN)	Percent Reduct'n below Stub Column
SP1	2.76	–	–	950.5	12.8	937.7	19.9
SP2	8.60	–	–	941.9	18.0	923.9	21.1
SP3	13.70	6.53	2.87	934.0	26.1	907.9	22.5
SP4	20.72	11.88	3.83	841.0	28.5	812.5	30.6
SP5	27.04	15.12	4.68	828.1	25.7	802.4	31.4
SP6	34.60	17.86	5.64	802.9	40.2	762.7	34.9
SP7	54.83	22.15	6.53	792.5	35.8	756.7	35.4
SP8	81.60	22.99	6.27	513.7*	32.7	481.0	–
SP9	22.2	27.4	29.5	840.0	–	–	–
SP10	24.51	13.94	4.36	1103.8	–	–	–
SP11	10.45	11.47	10.36	1620.0	–	–	–
Stub Column	–	–	–	1170.0	–	–	–

* Panel not loaded to ultimate

Sliding
Column

Fixed
End

} Subassembly selected
  for Testing

Cable in Bottom
Chord Tube

Sliding Joints Open

(a) Assembled at Ground Level

Sliding Joint Locked

(b) Stressed into Final Erected Position

FIG.1   STRARCH ERECTION CONCEPT

W_D

During erection, base free
to move horizontally

L
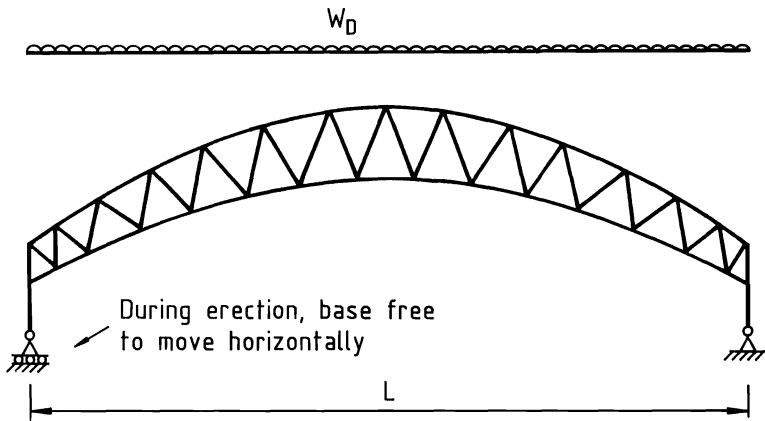
(a) Complete Strarch During Erection

W_D

M_{TC} ← C

→ T

h_C

h_T
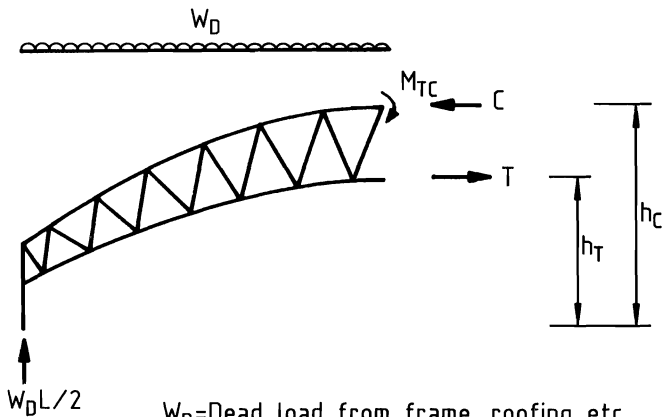
$W_D L/2$

W_D = Dead load from frame, roofing etc.
M_{TC} = Moment induced in top chord from lifting operation
    No moment assumed in bottom chord

Statics $\Rightarrow$ $C = T = \dfrac{\left(\dfrac{W_D L^2}{8} + M_{TC}\right)}{(h_C - h_T)}$

(b) Statics of Left Hand Section

FIG.2 STATICS OF STRARCH DURING ERECTION

Test panel positioned in horizontal plane

Fixed End Block

Hydraulic Supply Pipes

Servo Valve

Control Lines from Instrument Panel

Extending Ram

Bearing

2000kN Jack

Extensometer

Tension Bars forming Reaction Frame

Extensometer Control Arm

End Block free to move
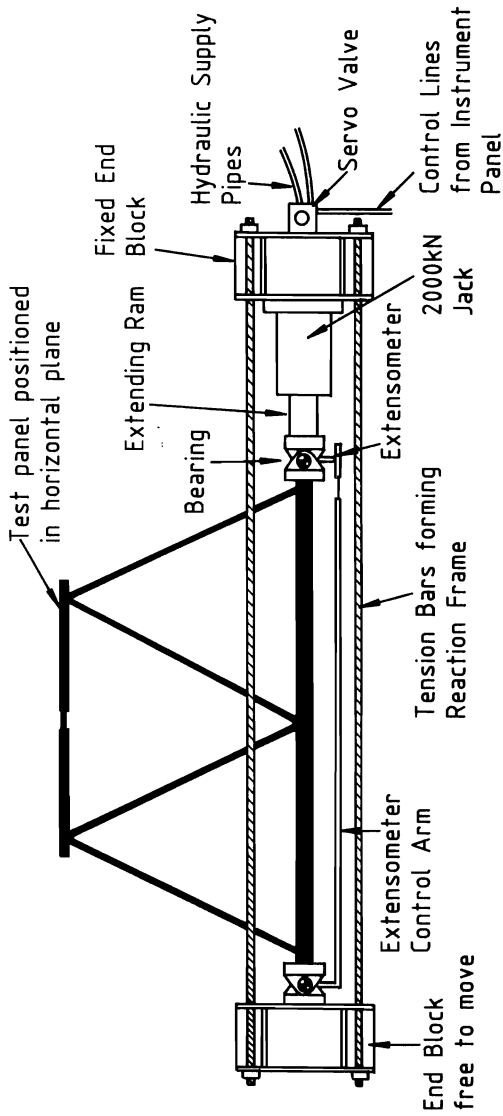
FIG.3   SCHEMATIC PLAN VIEW OF TEST RIG AND TEST PANEL

Initial Configuration:-

Test Panel (Type A or Type B)
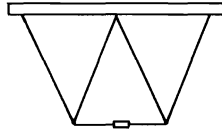
Stage 1:

Apply required curvature to top chord
by closing bottom chord sliding joint

δ
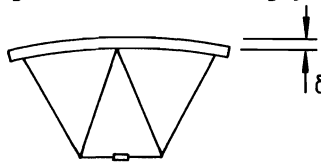
Stage 2:

Lock bottom chord sliding joint at required curvature
Apply jack load P_j to top chord using servo controlled
DARTEChydraulic loading ram

P_j —→   ←— P_j
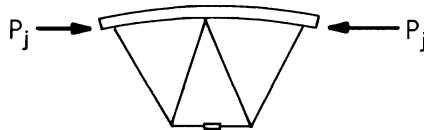
FIG.4   STRARCH PANEL TEST PROCEDURE
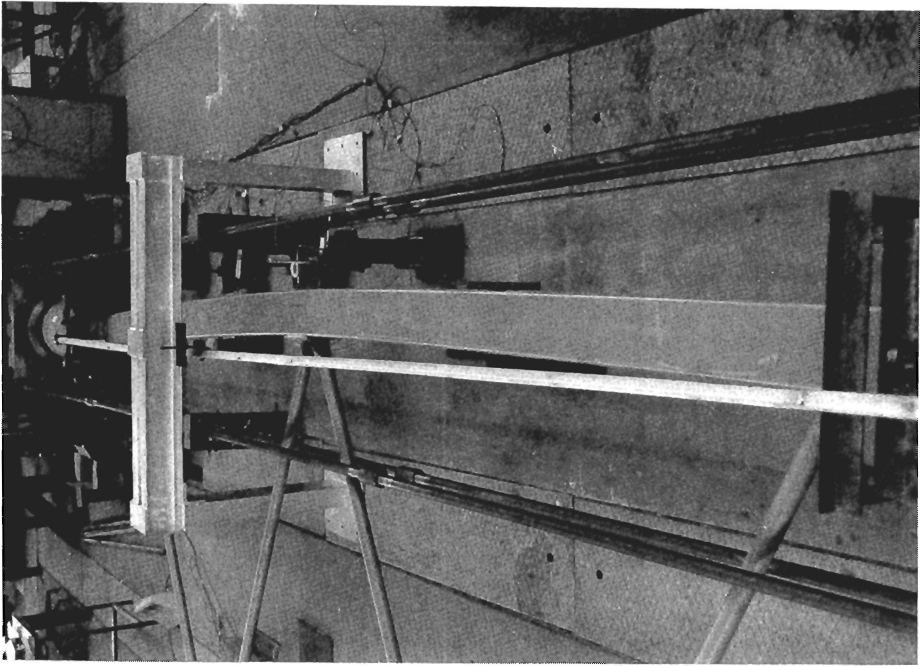
FIG.5(b) PANEL SP7 WITH FINAL CURVATURE
APPLIED TO TOP CHORD
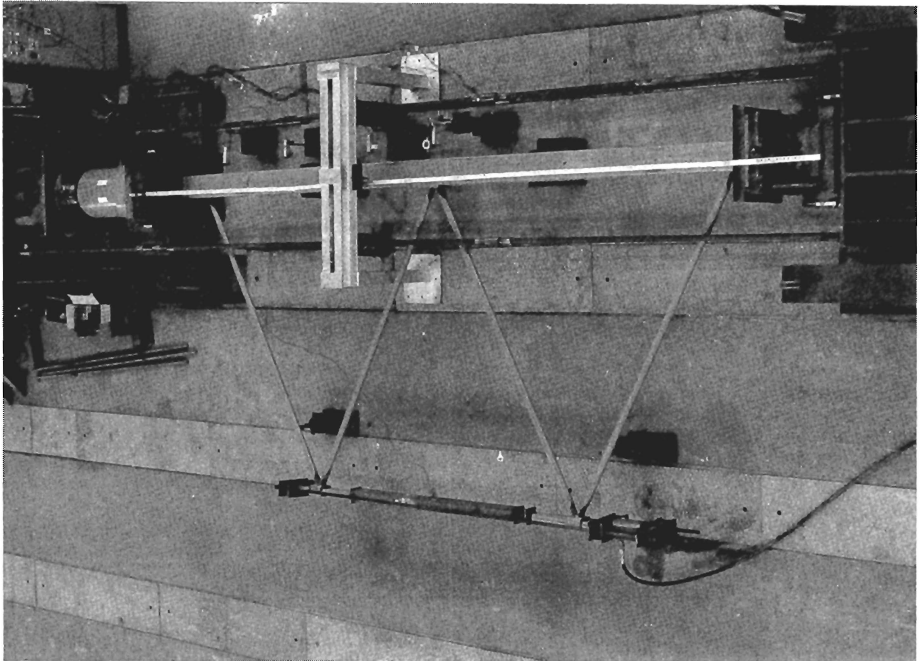
FIG.5(a) OVERHEAD VIEW OF TEST FRAME IN
LONG COLUMN TESTING RIG
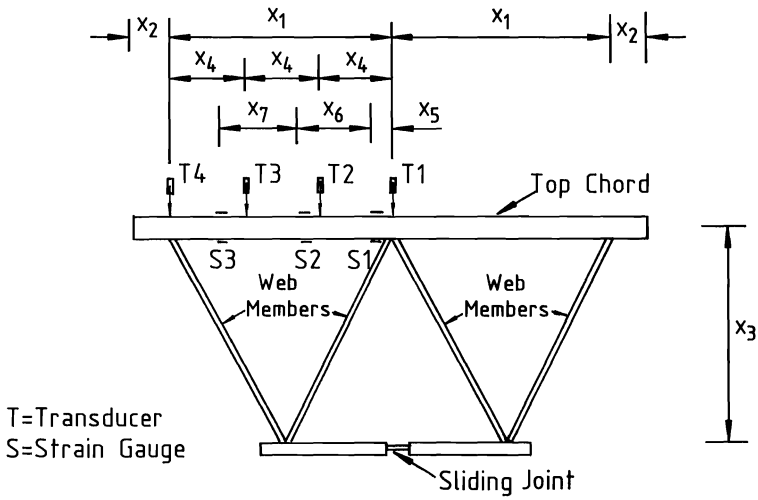
(a) Test Panel Type A
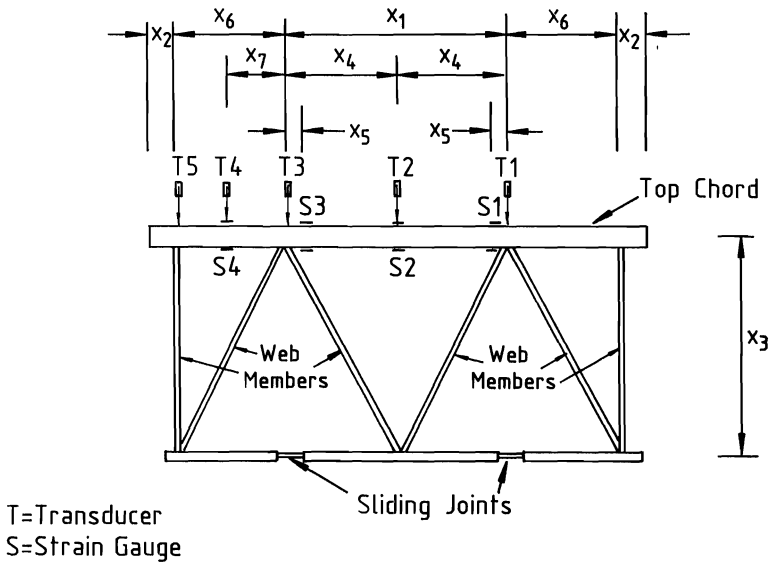
(b) Test Panel Type B

FIG.6   TEST PANEL GEOMETRY AND INSTRUMENTATION
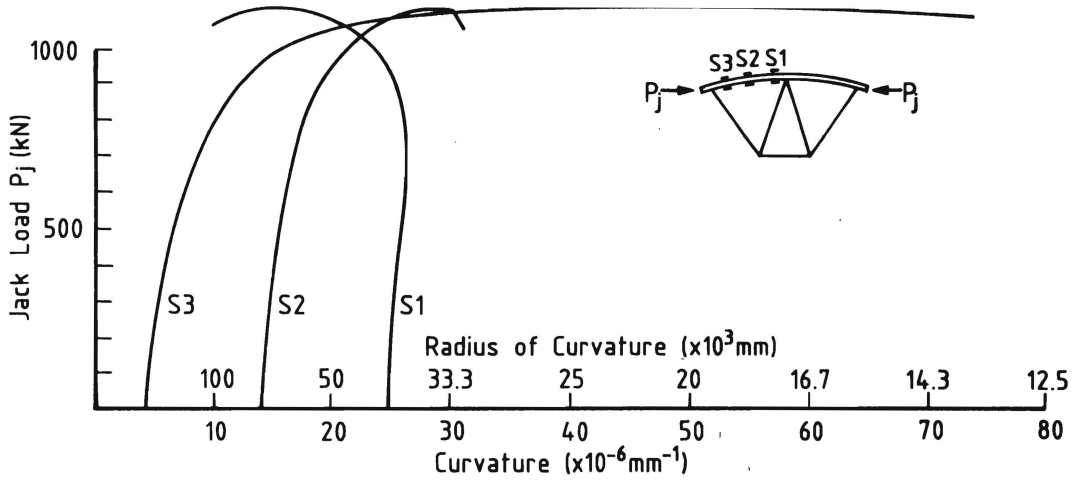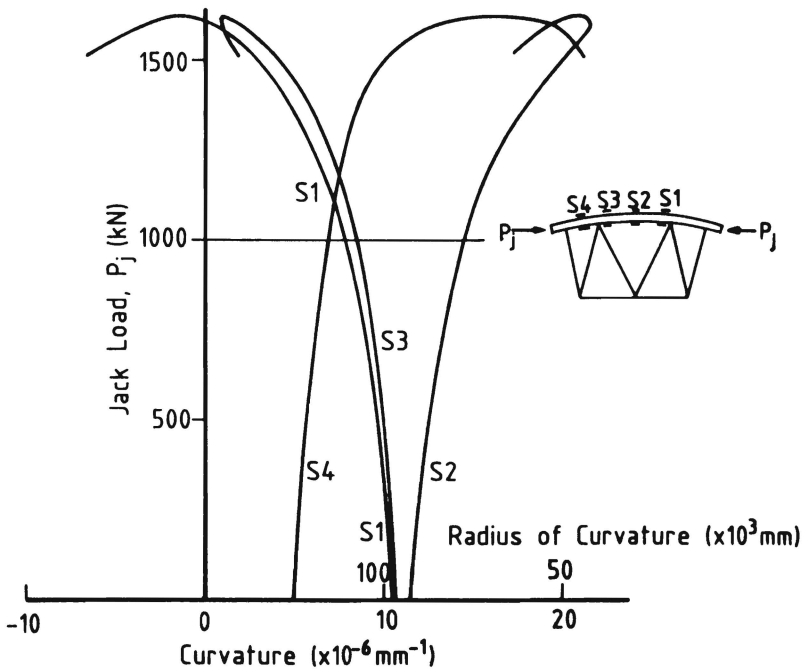
FIG.7(a) LOAD-CURVATURE PLOT - PANEL SP10 - δ=30mm
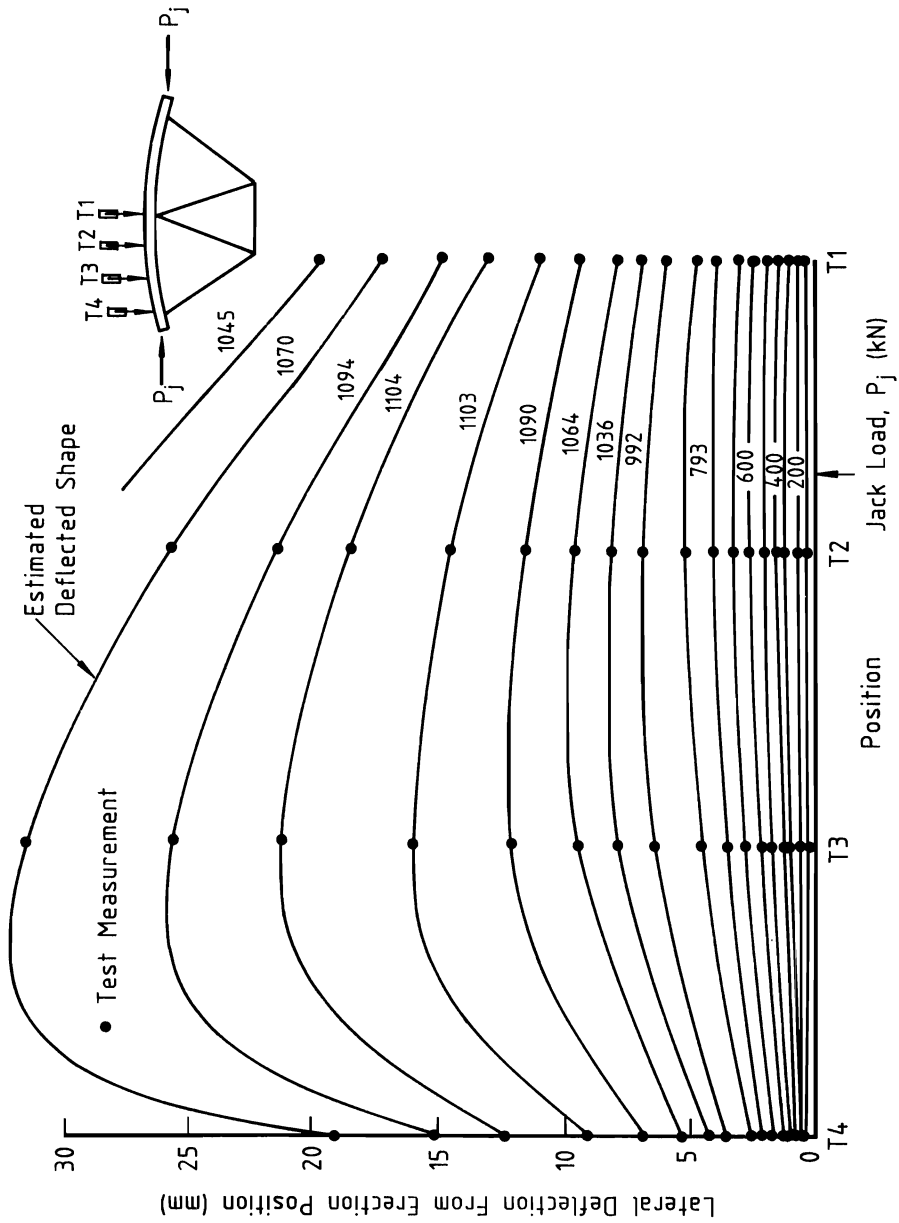

FIG.7(b) LOAD-CURVATURE PLOT - PANEL SP11

FIG.8(a) LATERAL DEFLECTION PROFILE – PANEL SP10 – δ=30mm

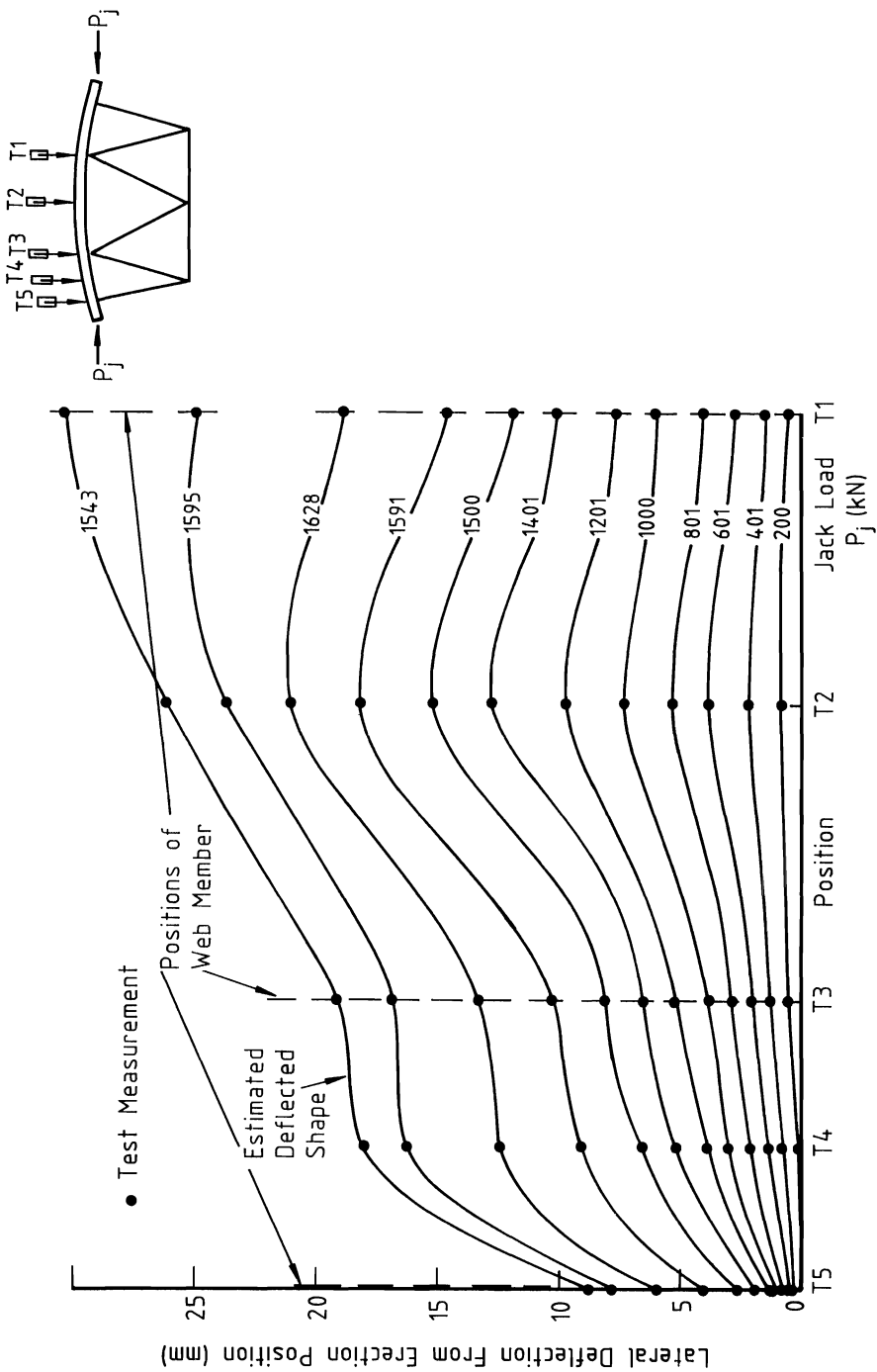FIG.8(b) LATERAL DEFLECTION PROFILE – PANEL SP11
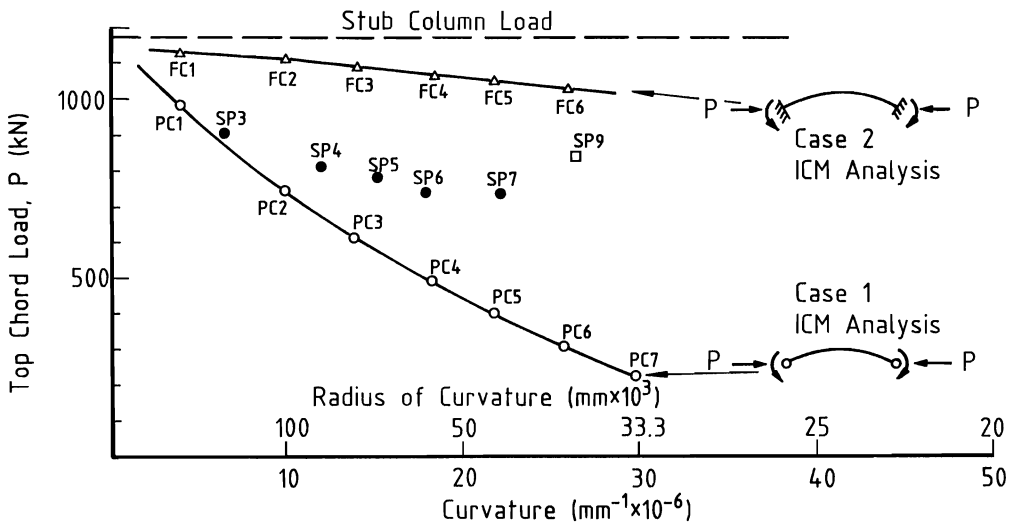
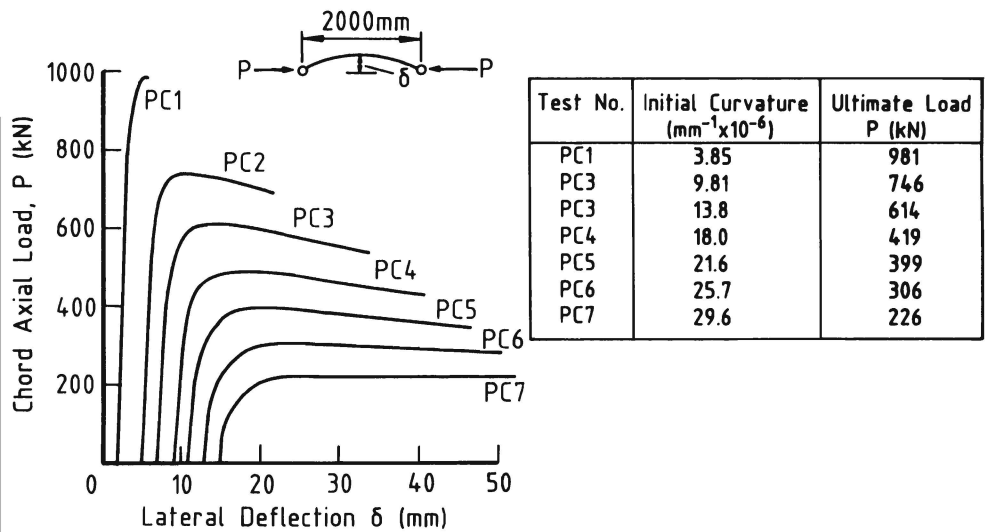FIG.9   COMPARISON OF ICM ANALYSIS WITH TEST RESULTS

FIG.10   ICM BEAM-COLUMN DISCRETIZATION

Test No.	Initial Curvature (mm⁻¹×10⁻⁶)	Ultimate Load P (kN)
PC1	3.85	981
PC3	9.81	746
PC3	13.8	614
PC4	18.0	419
PC5	21.6	399
PC6	25.7	306
PC7	29.6	226
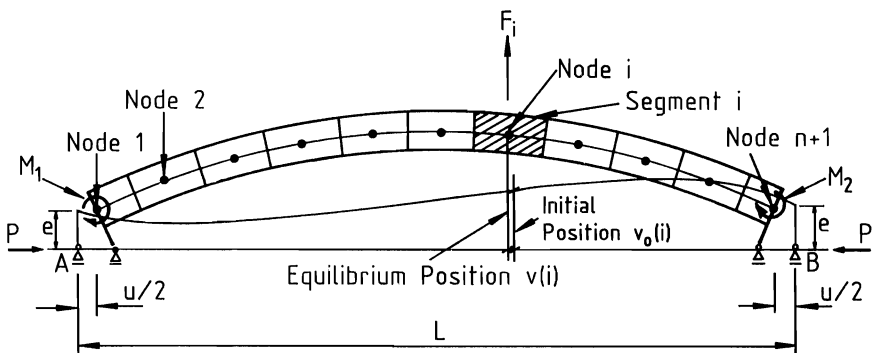
FIG.11(a)   AXIAL LOAD VS LATERAL DISPLACEMENT
STRARCH TOP CHORD - CASE 1

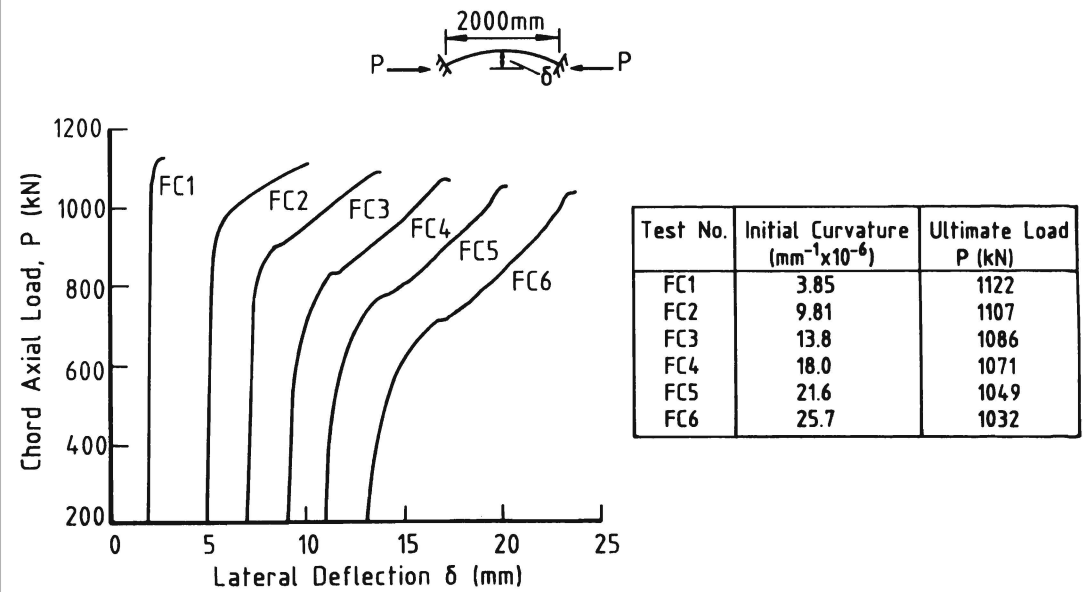| Test No.	Initial Curvature (mm⁻¹×10⁻⁶)	Ultimate Load P (kN)
FC1	3.85	1122
FC2	9.81	1107
FC3	13.8	1086
FC4	18.0	1071
FC5	21.6	1049
FC6	25.7	1032

FIG.11(b)   AXIAL LOAD VS LATERAL DISPLACEMENT
STARCH TOP CHORD - CASE 2